

## Influence of TiO<sub>2</sub> Nanoparticle Size on Electron Diffusion and Recombination in Dye-Sensitized TiO<sub>2</sub> Solar Cells

S. Nakade, Y. Saito, W. Kubo, T. Kitamura, Y. Wada, and S. Yanagida\*

Material and Life Science, Graduate School of Engineering, Osaka University, Suita, Osaka 565-0871, Japan

Received: March 26, 2003; In Final Form: May 28, 2003

Nanoporous electrode films are prepared from different sized anatase TiO<sub>2</sub> nanoparticles, of which the average diameter is 14, 19, and 32 nm. Dye-sensitized solar cells are prepared from the films. Diffusion coefficients of electrons ( $D$ ) in the solar cells are estimated by photocurrent transient measurements using a small-intensity laser pulse under continuous irradiation of bias light. Electron recombination lifetimes ( $\tau$ ) in the solar cells are measured by intensity-modulated photovoltage measurement (IMVS). It is found that the  $D$  increases and  $\tau$  decreases with the increase of the particle size up to 32 nm. The increase of the  $D$  is interpreted with the decrease of the film surface area, where the charge trap sites are likely to exist, and the condition of grain boundary. The decrease of  $\tau$  is discussed with the change of surface area and  $D$  with the particle size.

### Introduction

Dye-sensitized solar cells (DSC) have been the subject of intense study because of their high conversion efficiency and unique structures.<sup>1</sup> The solar cells consist of a dye-adsorbed nanoporous metal-oxide film filled with an electrolyte. The nanoporous film is prepared from typically nanosize particles of TiO<sub>2</sub> on a transparent conductive glass, and the electrolyte contains redox couples and several species of cations. Under light irradiation, charge separation occurs at the dye/TiO<sub>2</sub> interface, where photoexcited electrons in the dyes are injected into the conduction band of TiO<sub>2</sub> and the holes in the dyes are filled by the redox couples. Because the electrons in the nanoporous film are generally surrounded by many more cations than the electrons, it has been considered that no large electric field gradient is in the film.<sup>2,3</sup> Hence, the electron transport in the film has been mainly described with diffusion.<sup>4–6</sup>

To collect photogenerated electrons, electrons must travel a certain distance in the film to reach the transparent conductive oxide (TCO) layer before charge recombination occurs. The diffusion lengths of electrons in DSC have been estimated by measuring  $D$  and  $\tau$ .<sup>7</sup> The observed  $D$  showed power-law dependence on the incident light intensity, and  $\tau$  showed inverse power-law dependence, resulting in weak dependence of diffusion lengths on the light intensity. To explain the observations of the power-law dependence for  $D$ , several groups have developed trapping models, which assume that intraband charge trap sites exist in the films and electrons travel through the events of trapping and detrapping.<sup>8,9,10</sup> Hence, the electron transport has been modeled by the density and distribution of the trap sites in the nanoporous films.

For electron recombination lifetime, several studies have been made by measuring the lifetime with different dyes,<sup>12</sup> TiO<sub>2</sub> surface treatments,<sup>13</sup> cations,<sup>14</sup> electrolytes,<sup>15</sup> applied bias,<sup>16</sup> and film annealing temperatures.<sup>17</sup> These studies showed that the electron recombination lifetime is largely influenced by the characteristics of nanoporous films, especially trap site distribution and density. This is because the electron transport rate,

determined by the traps, could be related with the probability to encounter holes or the energy level of surface trap sites may determine the electron lifetime as described by the Shockley–Read model<sup>18,19</sup> or both. In addition to these, the electron recombination kinetics is further complicated because the species of redox couples has also significant effects on the lifetime. Several reports have interpreted that the observed long recombination lifetime with the I<sup>–</sup>/I<sub>3</sub><sup>–</sup> redox couple is attributed to the second-order reaction,<sup>7,13,20</sup>

For the DSC, holes are not generated in the nanoporous film. Hence, charge recombination occurs only with dye cations or I<sub>3</sub><sup>–</sup> in the electrolyte or both when the electrons meet them at the surface of particles. Thus,  $\tau$  could be influenced by the nanoporous film surface area, which determines effective electron acceptor density for the recombination. However, few studies have concerned the particle size in DSC as a parameter affecting  $\tau$ .

Previously, we studied the influence of nanoparticle preparation methods on  $D$  and  $\tau$  because the difference of the methods would change the trap site density and distribution. It was found that the conditions of nanoparticle surface and boundaries between particles, where the trap sites are likely to exist, largely affected  $D$ .<sup>11</sup> In the report, the influence of the particle size on diffusion coefficient was postulated. However, we could not show the effect directly because two parameters, surface condition and particle size, were different among the prepared samples and these effects could not be ruled out from each other. The aim of this paper is to study the influence of particle size in DSC on  $D$  and  $\tau$ . To have different sizes of TiO<sub>2</sub> particles with similar surface condition and crystallinity, nanoparticles were synthesized from the same starting materials and method. To interpret the measured  $D$  and  $\tau$ , we consider the location of charge traps. The implications of particle size to solar cell efficiency are also discussed.

### Experiments

Three different sizes of TiO<sub>2</sub> nanoparticles were prepared from hydrolysis of aqueous TiCl<sub>4</sub> solution, followed by autoclaving.<sup>21</sup> The particle size was changed by controlling the

\* To whom correspondence should be addressed. E-mail: yanagida@mls.eng.osaka-u.ac.jp.

temperature and time duration of the autoclaving. Colloidal suspensions were prepared from these particles dispersed in distilled water with PEG. To prepare thick films, 10 wt % of large TiO<sub>2</sub> particles (Ishihara Sangyo, ST-41, 200 nm in diameter) were mixed in the colloidal suspension to avoid cracks caused by a contraction of volume in the process of sintering.<sup>22</sup> Nanoporous films were prepared by dropping the suspension on a transparent conductive glass (Nippon Sheet Glass, SnO<sub>2</sub>: F, 8 Ω/sq) with using the doctor blade technique. The films were annealed at 550 °C for 30 min in air. The film thickness was measured with a profiler (Sloan, Dektak3). The surface area and porosity of the nanoporous films were measured by a nitrogen absorption apparatus (Quantachrome, Autosorb-1). Crystalline phase and size of the particles were analyzed with X-ray diffraction pattern with Cu Kα radiation ( $\lambda = 1.54$  Å) obtained from an X-ray diffraction (XRD) spectrometer (Rigaku RU-200B).

For photosensitization studies, the TiO<sub>2</sub> films were immersed in an ethanolic solution containing 0.3 mM Ru-dye, (*cis*-dithiocyanate-*N,N'*-bis(4-carboxylate-4-tetrabutylammoniumcarboxylate-2,2'-bipyridine) ruthenium(II) (known as N719, Solaronix), for 12 h at room temperature, and subsequently, the films were rinsed with acetonitrile. A thin platinum layer on a transparent conducting glass was used as a counter electrode. The redox electrolyte was prepared with 0.1 M LiI, 0.05 M I<sub>2</sub>, 0.6 M 1,2-dimethyl-3-propylimidazolium iodide, and 0.5 M 4-*tert*-butylpyridine in methoxy acetonitrile. Solar cells were prepared by placing a TiO<sub>2</sub> film on the counter electrode, and the electrolyte was introduced from the edge.

Electron diffusion coefficients of the films were measured using photocurrent transients induced by small-intensity laser pulse superimposed on bias light. Solar cells were irradiated by a short pulsed laser (Quanta-Ray, Nd:YAG, 7 ns,  $\lambda = 532$  nm) from the platinum electrode side. An aperture was placed in front of the cells, selecting irradiating area to be 0.093 cm<sup>2</sup>. During the measurements, a HeNe laser (Melles Griot,  $\lambda = 632.8$  nm) continuously irradiated the solar cells from the substrate side. The dyes absorb the wavelength very weakly so that nearly homogeneous electron density in the film was expected. The laser spot was defocused to obtain the same spot size as that of the pulsed laser. Intensity of both lasers was controlled by ND filters. Current transients were recorded by a digital oscilloscope with a current preamplifier (Stanford Research System, SR570). Electron diffusion coefficients were estimated by fitting a decay of the current transient with  $\exp(-t/\tau_c)$ , where  $t$  is time and  $\tau_c$  is a time constant, and then using<sup>10</sup>

$$D = w^2/(2.35\tau_c) \quad (1)$$

where  $w$  is the film thickness. For these measurements, the solar cells contained 10 wt % of large particles, and the edges of the solar cells were sealed by adhesive film (HIMILAN 1652, Mitsui-Dupont Polychemical) on a hot plate of a temperature of about 110 °C.

Electron recombination lifetimes in DSC were measured by intensity-modulated photovoltage spectroscopy (IMVS). The theory of the measurement was documented elsewhere.<sup>13</sup> The solar cells were irradiated by a diode laser (Coherent, LabLaser,  $\lambda = 635$  nm) from the substrate side. A fraction of the laser intensity (about 4% of steady intensity) was modulated with frequency ranging between 100 and 0.1 Hz. The photovoltage responses of the solar cells to the modulated light were measured. The modulation and measurements were operated by

**TABLE 1: Preparation Conditions and Characteristics of Nanoporous Films**

sample ID	autoclave temp, °C	autoclave time, h	size, nm	porosity, %	no. of particles/cm <sup>3</sup>	BET, m <sup>2</sup> g <sup>-1</sup>
S14	180	2	14	59	$2.8 \times 10^{17}$	90
S19	240	2	19	55	$1.2 \times 10^{17}$	63
S32	240	24	32	51	$0.28 \times 10^{17}$	48

a LCR meter (Hioki, 3522 LCR Hitester) with a voltage amplifier (NF Electronic Instruments, 3507 differential amplifier). Short-circuit current ( $I_{sc}$ ) and open-circuit voltage ( $V_{oc}$ ) were measured with a digital multimeter (Keithley 196 system DMM). The  $I_{sc}$  was measured before and after the IMVS measurements to check whether the cells maintained a steady condition during the measurements. Note that the films used for IMVS did not contain the large particles.

## Results

**Film Characterization.** Table 1 summarizes particle synthesis conditions and characteristics of the nanoporous films prepared from the particles. Hereafter, the sample ID on the table will be used to refer to the samples. Particles were prepared also at the autoclaving temperature of 240 °C for 72 h, resulting in the 34-nm-size particles. Here, we chose 32-nm-size particles resulted from 24 h autoclaving as the largest sample from the method. For the smallest sample, because 2 h of autoclaving at 240 °C gave 19-nm-size particles, a lower temperature was used. All peaks of XRD patterns obtained from these three samples showed the agreement of the reference data of anatase. The particle sizes were estimated with Sherrer's equation using a peak at  $2\theta = 25.4^\circ$  and scanning electron microscopy (SEM) observations. Figure 1 shows SEM images of these samples. The estimated crystal sizes from the XRD peaks were 14, 18, and 25 nm, which correspond 14, 19, and 32 nm from SEM observations, respectively. This suggests that the particles probably consist of single crystal,<sup>11</sup> and S32 may have a higher portion of surface amorphous state or a wider distribution of particle size than the others or both.<sup>23</sup> For porosity, the film consisting of the largest particles showed the lowest porosity. The numbers of particles in the films were estimated with the particle size and the porosity, as shown in Table 1. The films consisting of 32-nm-size particles have about  $1/10$  of particles in the films of 14-nm-size particles per unit volume.

**Electron Diffusion Coefficients in DSC.** Figure 2 shows current transients induced by a small-intensity laser pulse under bias light. The solar cell used here consisted of 19-nm-size particles with the thickness of 4.9 μm. Three transients on the figure were obtained by different bias light intensities as indicated by  $I_{sc}$  generated by the bias light. Excess electron densities induced by a pulse were estimated by integrating corresponding current transient to be on the order of  $10^{14}$ – $10^{15}$ /cm<sup>3</sup>, which were much smaller than that obtained by the bias light. The decays of the transients were fitted by an exponential function with a single time constant. The fitted time constant showed an increase with decreasing bias light intensity, corresponding to electrons that spent longer time to reach the TCO. The measurements and fitting were repeated several times under the same bias intensity. The deviation of the fitted time constant was about 10%. The measurements were also performed for other samples consisting of 14- and 32-nm-size particles under various bias light intensities, and the electron diffusion coefficients were estimated by eq 1. The estimated diffusion coefficients from the fitted time constant are plotted in Figure

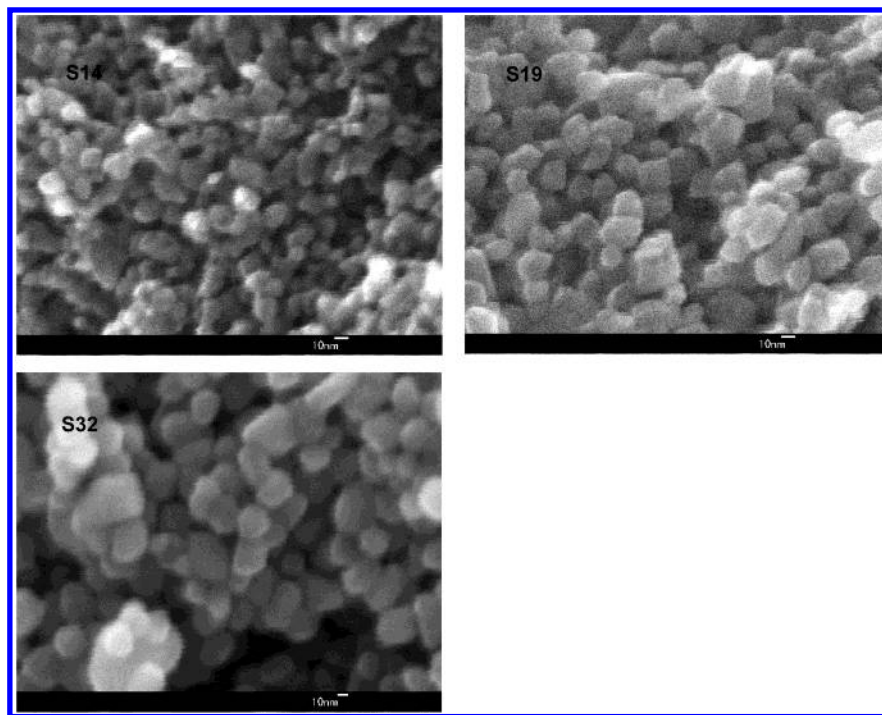


**Figure 1.** SEM images of TiO<sub>2</sub> nanoporous films, prepared from three different TiO<sub>2</sub> nanoparticles. XRD patterns showed that all samples are anatase. Average particle size is 14 nm for S14, 19 nm for S19, and 32 nm for S32.

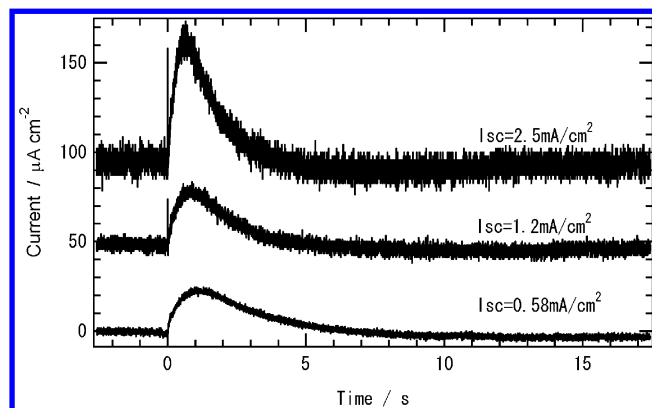


**Figure 2.** Current transients from DSC induced by a laser pulse of small intensity superimposed on bias light. The sample is made from a 4.9  $\mu\text{m}$  thick TiO<sub>2</sub> film consisting of 19-nm-size particles.

3 as a function of  $I_{\text{sc}}$  per TiO<sub>2</sub> unit volume obtained from short-circuit current divided by film thickness and one minus porosity. The film thicknesses of the samples were nearly the same, as indicated on the figure caption. As it is seen, the diffusion coefficients increase with the particle size. In the plot, all samples showed nearly power-law dependence on  $I_{\text{sc}}$ .

**Electron Recombination Lifetime in DSC.** IMVS measurements of all of the samples showed a semicircle on a plot of  $\text{Re}(\Delta V)$  vs  $\text{Im}(\Delta V)$ , which was similar to the previously reported results by others.<sup>7,13</sup> Hence, electron recombination lifetimes at open circuit were estimated from the frequency ( $f$ ) giving the minimum of the semicircle using  $\tau = 1/(2\pi f)$ .<sup>7,13</sup> The obtained electron lifetime in the solar cells as a function of  $I_{\text{sc}}$  per TiO<sub>2</sub> unit volume is shown in Figure 4. The error bars in the figure are the deviation of the results from four samples or less.<sup>24</sup> All films showed the decrease of  $\tau$  with the increase of the bias light intensity. The tendency and the order of  $\tau$  are similar to the results from other groups.<sup>7,17</sup> As it is seen, the recombination lifetime decreases with the increase of the particle size.

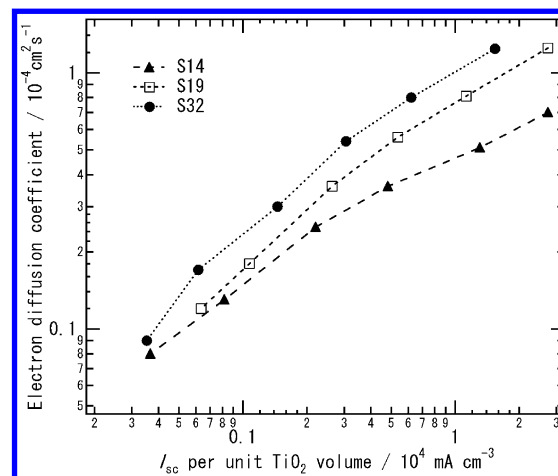


**Figure 3.** Diffusion coefficients of electrons in DSC consisting of different size particles as a function of  $I_{\text{sc}}$  per unit TiO<sub>2</sub> volume generated by the bias light. Thicknesses of the films used here were 4.7  $\mu\text{m}$  for S14, 4.9  $\mu\text{m}$  for S19, and 4.8  $\mu\text{m}$  for S32.

## Discussion

**Particle Size and Electron Diffusion Coefficient.** Diffusion coefficients of electrons in nanoporous films have been interpreted mainly with charge trap site distribution and the trap density. The charge trap sites may be formed by crystal defects, impurities, surface amorphous layer, and chemical surroundings. The traps would be located mainly on the surface of the particles because of the high surface ratio to volume in the nanosized TiO<sub>2</sub>. This was also suggested by some experimental results.<sup>25</sup>

Table 2 summarizes  $D$  at the electron density of  $8 \times 10^{16} \text{ cm}^{-3}$  in the films estimated by multiplying  $I_{\text{sc}}$  and transit time divided by the film thickness and one minus porosity. On the basis of the trapping model,  $D$  relates inverse proportionally to the number of traps. Assuming that the traps are located at the surface of particles,  $D$  should scale with  $r^{2/3}$ , where the  $r$  is the radius of nanoparticles. If the number of traps is rather proportional to the number of grain boundaries,  $D$  should scale



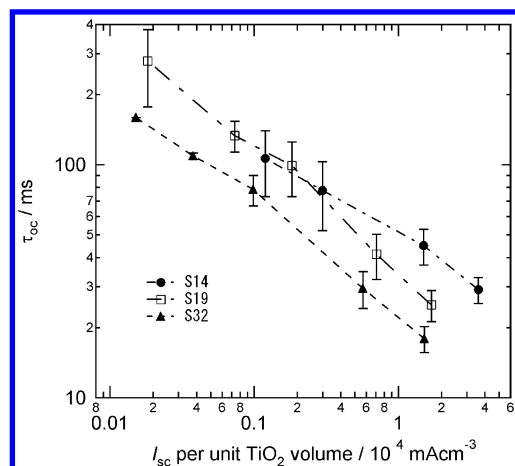


**Figure 4.** Electron recombination lifetimes at open-circuit condition in DSC consisting of different size particles. The lifetimes were estimated by IMVS.

**TABLE 2: Comparison of  $D$  and  $\tau$  in DSC Prepared from Different Sized  $\text{TiO}_2$  Nanoparticles<sup>a</sup>**

size, nm	lifetime, ms	$D$ , $10^{-4} \text{ cm}^2 \text{ s}^{-1}$	BET area, $\text{m}^2 \text{ g}^{-1}$	$D/r^3$ , au	$D/r^{2/3}$ , au
14	70	0.33	90	9.6	0.90
19	40	0.78	63	9.1	1.7
32 (25)	18	1.2	48	2.9 (6.1)	1.9 (2.2)

<sup>a</sup> The  $D$  were chosen at the electron density in the  $\text{TiO}_2$  electrode of  $8 \times 10^{16} \text{ cm}^{-3}$ , and  $\tau$  were chosen at corresponding light intensity. The numbers in parentheses show the cases for 25 nm size.

with  $r^3$ .<sup>26</sup> Table 2 includes constant numbers for these two cases. From the table, it is difficult to conclude the contribution of the trap site location. And, this result implies that another factor affecting  $D$  needs to be considered.

In addition to the trap sites, the conditions of grain boundaries can also change the  $D$ .<sup>27</sup> Because lattice mismatch is at the boundaries, electron transport rate should be affected by the conditions such as the thickness and the cross-sectional area of the boundary. When the particle size becomes nanosize order, the volume of material used for boundaries in a film cannot be ignored. The volume ratio of boundaries to particles was estimated to be 30–50% when the particle size is 10 nm with a 1–2 nm thick boundary.<sup>28</sup> For these cases, describing electron transport in such films requires taking account of the electron transport in both boundary and crystal. One possible explanation of Table 2 is that  $D$  scales with  $r^{2/3}$  and the influence of the grain boundaries appears more significantly as the particle size decreases.

**Particle Size and Electron Recombination Lifetime.** Recombination of electrons and holes/electron acceptors in DSC should occur at the interface between the nanoporous film and the electrolyte. There have been arguments whether the electrons recombine through surface trap sites or directly from the conduction band. If the measured lifetime is shorter than the required time to escape from trap sites, then the recombination path is mostly through the trap sites. However, the analysis of the experimental results in the literature showed that most electrons repeat thousands of trapping/detrapping events,<sup>10</sup> making it difficult to rule out the possible recombination paths. At this moment, light-intensity dependence of the lifetime has been mainly interpreted with a trapping model or a second-order reaction of  $\text{I}^-/\text{I}_3^-$  couple or both.

When the surface area is decreased, the effective electron-acceptor concentration should be decreased. Then, a longer

recombination lifetime with the increase of the particle size was expected. If the recombination occurs through the surface trap sites, this case also predicts a longer lifetime with the decrease of the surface area. However, the observed lifetimes were opposite. An alternative explanation of the shorter  $\tau$  with the increase of particle size is caused by the increase of the  $D$ , that is, the rate to meet holes is related to the frequency of hopping between traps. Here, we could not relate with how the two-electron redox system used here affects our observation while the redox system also affects the recombination lifetime significantly.<sup>29</sup> To substantiate the mechanism of the electron recombination further, the measurement of  $\tau$  using a one-electron redox system as proposed by Peter et al. would be one approach.<sup>30</sup> In addition to this, the measurement of  $\tau$  with various concentrations of cations in electrolytes would also reveal the relationship between  $D$  and  $\tau$ . This is because the  $D$  can be controlled by the concentration of cations without changing other conditions.

**Implications for the DSC.** Based on the measurements of  $D$  and  $\tau$ , electron diffusion lengths in the nanoporous films having different sizes of nanoparticles are in the same order. To optimize the particle size to increase  $I_{\text{sc}}$ , smaller particles seem beneficial to increase the effective light absorption coefficients of the solar cells, which increase the amount of photogenerated electrons close to TCO. However, our results showed small particles, for example, S14, may result in the shorter diffusion length. In addition to the diffusion length issue, a recent report revealed that charge injection efficiency was also lowered with the decrease of the particle size.<sup>31</sup> On the other hand, increasing particle size may not increase diffusion length enough to compensate for the decrease of the effective light absorption coefficients due to the decrease of the surface area.

## Conclusions

Electron diffusion coefficients and recombination lifetimes in nanoporous  $\text{TiO}_2$  films were studied with the size of particles and the film surface area. It was found that diffusion coefficient increased with particle size among the samples prepared from the same starting materials. The increase was related to the decrease of the film surface area and the condition of grain boundaries. Measured values of electron recombination lifetimes in DSC were decreased with increase of the particle size. The results implied that the recombination lifetime was related to the electron transport rate in the  $\text{TiO}_2$  electrodes. For designing solar cells, these studies show that there is an optimized particle size to obtain the highest electron-harvesting efficiency.

**Acknowledgment.** This work was partially supported by Grant-in-Aid for Scientific Research (Grant No. 11358006) and Open Competition for the Development of Innovative Technology (Grant No. 12310) in Grant-in-Aid for the Creation of Innovations through Business-Academic-Public Sector Cooperation from the Ministry of Education, Culture, Sports, Science and Technology of Japan. The authors thank the referee for the helpful suggestions during the review processes.

## References and Notes

- O'Regan, B.; Grätzel, M. *Nature* **1991**, *353*, 737.
- Schwarzburg, K.; Willing, F. *J. Phys. Chem. B* **1999**, *103*, 5743.
- van de Lagemaat, J.; Park, N.-G.; Frank, A. J. *J. Phys. Chem. B* **2000**, *104*, 2044.
- Södergren, S.; Hagfeldt, A.; Olsson, J.; Lindquist, S.-E. *J. Phys. Chem.* **1994**, *98*, 5552.
- Cao, F.; Oskam, G.; Meyer, G. J.; Searson, P. C. *J. Phys. Chem.* **1996**, *100*, 17021.

- (6) Solbrand, A.; Lindström, H.; Rensmo, H.; Hagfeldt, A.; Lindquist, S.-E. *J. Phys. Chem. B* **1997**, *101*, 2514.
- (7) (a) Fisher, A. C.; Peter, L. M.; Ponomarev, E. A.; Walker, A. B.; Wijayantha, K. G. U. *J. Phys. Chem. B* **2000**, *104*, 949. (b) Peter, L. M.; Wijayantha, K. G. U. *Electrochem. Commun.* **1999**, *1*, 576.
- (8) Nelson, J. *Phys. Rev. B* **1999**, *59*, 15374.
- (9) de Jongh, P. E.; Vanmaekelbergh, D. *Phys. Rev. Lett.* **1996**, *77*, 3427.
- (10) van de Lagemaat, J.; Frank, A. J. *J. Phys. Chem. B* **2001**, *105*, 11194.
- (11) Nakade, S.; Matsuda, M.; Kambe, S.; Saito, Y.; Kitamura, T.; Sakata, T.; Wada, Y.; Mori, H.; Yanagida, S. *J. Phys. Chem. B* **2002**, *106*, 10004.
- (12) Tachibana, Y.; Haque, S. A.; Mercer, I. P.; Durrant, J. R.; Klug, D. R. *J. Phys. Chem. B* **2000**, *104*, 1198.
- (13) Schlichthörl, G.; Huang, S. Y.; Sprague, J.; Frank, A. J. *J. Phys. Chem. B* **1997**, *101*, 8141.
- (14) Pelet, S.; Moser, J.-E.; Grätzel, M. *J. Phys. Chem. B* **2000**, *104*, 1791.
- (15) Nelson, J.; Haque, S. A.; Klug, R. D.; Durrant, J. R. *Phys. Rev. B* **2001**, *63*, 205321.
- (16) Haque, S. A.; Tachibana, Y.; Willis, R. L.; Moser, J. E.; Grätzel, M.; Klug, D. R.; Durrant, J. R. *J. Phys. Chem. B* **2000**, *104*, 538.
- (17) Park, N.-G.; Schlichthörl, G.; van de Lagemaat, J.; Cheong, H. M.; Mascarenhas, A.; Frank, A. J. *J. Phys. Chem. B* **1999**, *103*, 3308.
- (18) Usami, A.; Ozaki, H. *J. Phys. Chem. B* **2001**, *105*, 4577.
- (19) Bisquert, J.; Zaban, A.; Salvador, P. *J. Phys. Chem. B* **2002**, *106*, 8774.
- (20) Gregg, B. A.; Pichot, F.; Ferrere, S.; Fields, C. L. *J. Phys. Chem. B* **2001**, *105*, 1422.
- (21) Saito, Y.; Kambe, S.; Wada, Y.; Kitamura, T.; Yanagida, S. *Sol. Energy Mater. Sol. Cells*, in press.
- (22) We have checked the influence of the 10 wt % addition of large particles, which are usually added for light scattering in the films, on  $D$  with different TiO<sub>2</sub> particles and found that no effect was seen in the accuracy of the measurement method. The effect on BET surface area was also measured, and the difference was less than 3% even with 20 wt % addition of the scattering particle.
- (23) Particle size might be estimated by BET area measurements. However, for the case of TiO<sub>2</sub> particles used in this work, the BET area depends on the film annealing temperature while the size estimated from XRD shows independent from the temperature (ref 11). Then, on the basis of the agreements between XRD and SEM data for smaller size particles, we rely on the size estimated by SEM for the large particles.
- (24) Data from some samples were not stable under very low bias light intensities. For this case, the data on the figure are based on the results from stable samples.
- (25) (a) Duffy, N. W.; Peter, L. M.; Rajapakse, R. M. G.; Wijayantha, K. G. U. *Electrochem. Commun.* **2000**, *2*, 658. (b) Wang, H.; He, J.; Boschloo, G.; Lindström, H.; Hagfeldt, A.; Lindquist, S.-E. *J. Phys. Chem. B* **2001**, *105*, 2529.
- (26) This discussion was kindly suggested by the referee.
- (27) Cass, M. J.; Qiu, F. L.; Walker, A. B.; Fisher, A. C.; Peter, L. M. *J. Phys. Chem. B* **2003**, *107*, 113.
- (28) Takagi, S. *Materia* **2002**, *6*, 418.
- (29) A simple equation to describe the recombination rate with hopping frequency is  $dn/dH = -Apn$ , where  $n$  is the electron density,  $p$  is the hole density,  $A$  is a constant, and  $H$  is a time for electrons to hop between traps (ref 15). The constant  $A$  can also control the time scale of the recombination lifetime, and it should depend on TiO<sub>2</sub> surface conditions and type of holes. In this work, we changed only the particle size so that we assume the  $A$  was the same for the all samples used here.
- (30) Peter, L. M.; Duffy, N. W.; Wang, R. L.; Wijayantha, K. G. U. *J. Electroanal. Chem.* **2002**, *524*, 127.
- (31) Benco, G.; Skarman, B.; Wallenberg, R.; Hagfeldt, A.; Sundstrom, V.; Yartsev, A. P. *J. Phys. Chem. B* **2003**, *107*, 1370.